Analytical Methods

Accepted Manuscript

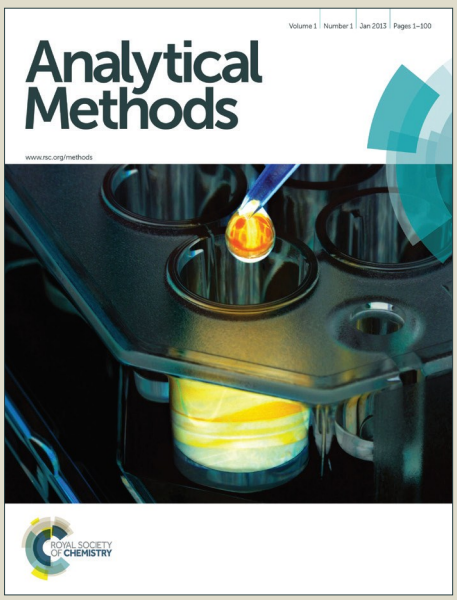

This is an *Accepted Manuscript*, which has been through the Royal Society of Chemistry peer review process and has been accepted for publication.

Accepted Manuscripts are published online shortly after acceptance, before technical editing, formatting and proof reading. Using this free service, authors can make their results available to the community, in citable form, before we publish the edited article. We will replace this *Accepted Manuscript* with the edited and formatted *Advance Article* as soon as it is available.

You can find more information about *Accepted Manuscripts* in the Information for Authors.

Please note that technical editing may introduce minor changes to the text and/or graphics, which may alter content. The journal's standard Terms & Conditions and the Ethical guidelines still apply. In no event shall the Royal Society of Chemistry be held responsible for any errors or omissions in this *Accepted Manuscript* or any consequences arising from the use of any information it contains.

ROYAL SOCIETY OF CHEMISTRY

www.rsc.org/methods

A sensitive enzyme-free hydrogen peroxide sensor based on chitosan-graphene quantum dots / silver nanocubes nanocomposite modified electrode

Yingying Jiang,[a] Yuhui Li,[a] Yancai Li[a,b,*] and Shunxing Li[a,b]

[a]College of Chemistry & Environment, Minnan Normal University, Zhangzhou 363000, P. R. China

[b]Fujian Province Key Laboratory of Modern Analytical Science and Separation Technology, Minnan Normal University, Zhangzhou 363000, P. R. China

*Corresponding author. Tel.: +86-596-2591445; Fax: +86-596-2520035

e-mail: liyancai@mnnu.edu.cn

Abstract: The graphene quantum dots (GQDs) and silver nanocubes (AgNCs) were synthesized successfully and characterized by UV-Vis and fluorescence (FL) spectra, Fourier transform infrared (FT-IR) spectroscopy, transmission electron microscopy (TEM) and scanning electron microscopy (SEM). The GQDs and AgNCs modified gold electrode (GE) possesses well conductivity by electrochemical impedance spectroscopy (EIS). The Chit-GQDs/AgNCs/GE displays good electrocatalytic activity towards the reduction of hydrogen peroxide (H_2O_2), and can be used as a novel and sensitive enzyme-free H_2O_2 sensor. According to the amperometric experiments, the sensor exhibits a rapid response, a wide linear range from 10 μM to 7.38 mM, a low detection limit of 0.15 μM and high selectivity, as well as good repeatability to H_2O_2 determination.

Keywords: Graphene quantum dots; silver nanocubes; electrocatalytic; enzyme-free sensor; hydrogen peroxide

1. Introduction

Hydrogen peroxide (H_2O_2) is an important analyte due to its excessive use in industry and atomic power stations, which dramatically affects the cloud and rainwater,[1] as well as one of the major risk factors in progression of pathophysiological

complications in diabetes, renal disease, cancer and aging.[2] Therefore, it is always very important to determinate H_2O_2 and develop H_2O_2 sensor. Up to now, various methods, including spectrometry,[3] titrimetry,[4] fluorimetry,[5] chemiluminescence,[6] surface plasmon resonance,[7] chromatography[8] and electrochemistry,[9] have been employed to determinate H_2O_2. Compared with other described methods, the electrochemical method is catching increasing attentions because of its superiority, such as convenient, rapid, good selectivity and sensitivity.[10] Usually, numerous heme proteins and enzymes modified electrodes, such as hemoglobin, myoglobin and horseradish peroxidase-based electrodes, are frequently used for electrocatalytic reduction of H_2O_2 and used as H_2O_2 biosensor.[11] However, the relatively high cost, limited lifetime and the critical operating situation limit the application of the protein or enzyme-based biosensors. Therefore, the development of nonenzymatic sensors with low detection limit has drawn more attention recently.[12, 13]

In recent years, with the rapid development of nanoscience and nanotechnology, metal and alloy nanomaterials have been widely used to design enzyme-free H_2O_2 sensors which gradually replace enzymes based H_2O_2 biosensors.[10] Metal nanoparticles(NPs), such as PtNPs,[12] AuNPs[14] and AgNPs[15] have been proposed as electrocatalysts to determine trace H_2O_2. Among various nanomaterials, Ag nanoparticles have been widely used in biosensing because of their superior performance such as catalysis, conductivity, stability and large surface area.[16] For example, Fang et al. fabricated an electrochemical H_2O_2 sensors based on Ag nanoparticles and graphene-polyelectrolyte brushes,[17] Habibi et al. reported the characterization of mesoporous carbon and silver nanoparticles (MC/AgNPs) to use in amperometric sensing of H_2O_2,[18] which both yielded good performance toward the detection of H_2O_2. Furthermore, it is well-known that the shape of metal nanoparticles is a key factor which influence the electrocatalytic activity of nanomaterials.[19, 20] Recent studies found that performance of the H_2O_2 sensor depended strongly on the size, shape and distribution of AgNPs on the electrode.[21] Therefore, Ag nanocubes which possess unique structural features and the own characteristics of silver, will display well electrocatalytic properties and have potential application in electrocatalyst and

biosensing.

Graphene quantum dots (GQDs), as recently emerging carbon-based materials, are graphene sheets smaller than 100 nm.[22] GQDs are superior in terms of low cytotoxicity, [23]excellent biocompatibility, simple synthesis and remarkable conductivity.[24] Furthermore, the GQDs contain many chemical groups such as hydroxyl, carbonyl, and carboxylic acid groups.[25] In addition, GQDs have some excellent characteristics, such as high surface area, larger diameter, better surface grafting using the π–π conjugation and other special physical properties due to the structure of graphene. [24] The early work on GQDs was dominated by the investigation of their preparation and physical properties. More recently, GQDs have been chemically modified and used in applications in the area of energy conversion, bioanalysis and sensors.[26] For example, Zhang et al. fabricated an electrochemical H_2O_2 sensors based on GQDs modified Au electrode, [27] Ju and Chen reported the in situ growth of surfactant-free AuNPs on N-GQDs to use in sensing of H_2O_2,[28] which both exhibit high sensitivity and low detection limit. Therefore, GQDs can be used as a candidate material for electrode modification and then used in electrochemical biosensing.

In this paper, combined with the advantages of AgNCs and GQDs, we synthesized and characterized the GQDs and AgNCs, and then developed a novel amperometric H_2O_2 sensor based on the immobilization of AgNCs and GQDs to gold electrode. The obtained H_2O_2 sensor shows a rapid response, a low detection limit, a wide linear range, high selectivity and good repeatability. The present work may expand the use of silver nanocubes (AgNCs) and GQDs in the field of electrochemical sensor.

2. Experimental

2.1 Reagents

Both PVP (K30, Mw=30000-40000) and silver nitrate were purchased from Sinopharm Chemical Reagent Co., Ltd. Chitosan (Deacetylation>95%) was obtained from Sanland Chemical Co., Ltd. Ethylene glycol (EG), citric acid and H_2O_2 (30 wt%) were purchased from Xilong Chemical Co., Ltd. (Guangdong, China). Phosphate buffer solution (PBS) was prepared by mixing 0.1 M NaH_2PO_4 and Na_2HPO_4. A chitosan

solution (0.5 wt.%) was prepared by dissolving 0.015g chitosan in 3mL acetic acid (v/v, 1%). All other chemicals were of analytical grade and were used without further purification. All solutions were made up with double-distilled water.

2.2 Apparatus

The morphology of the AgNCs was analyzed via scanning electron microscopy (SEM) on the Hitachi S-4800 instrument (Hitachi, Tokyo, Japan). Transmission electron microscopy (TEM) was performed on a JEM-1230 electron microscope (JEOL, Ltd., Japan) at 300 kV. Fourier transforms infrared spectroscopy (FT-IR) was recorded on a Bruker IFS66V FT-IR spectrometer. Ultraviolet visible (UV-vis) absorption spectra were recorded by Mapada UV-1800PC (Shanghai Mapada Instruments Co., Ltd, China). The fluorescence spectra were obtained by a Varian Cary Eclipse Fluorescence Spectrophotometer (Agilent Technologies, Santa Clara, America) with a 1.0 cm quartz cell (Ex slit 10 nm, Em slit 10 nm). Electrochemical experiments were performed with a CHI650D electrochemical workstation (Shanghai Chenhua Instrument Co., Ltd) with a conventional three-electrode cell. A bare or modified gold electrode (GE) was used as working electrode, Ag/AgCl (3.0 M KCl) and platinum wire was used as reference electrode and auxiliary electrode, respectively. All experiments were conducted at the ambient temperature. Prior to the experiment, the PBS was purged with high-purity nitrogen for at least 30 min and a nitrogen atmosphere was maintained over the solution.

2.3 Synthesis of GQDs and AgNCs

The GQDs were synthesized by a convenient method according to anteriorly reported method.[29] In a typical procedure of GQDs preparation, 2 g of citric acid was put into a 5 mL beaker, and heated to 200 °C by a heating mantle for about 30 min until the citric acid changed to an orange liquid. Then, the liquid was dissolved into 100 mL of 10 mg mL^{-1} NaOH solution drop by drop, with continuous and vigorous stirring. The obtained GQDs solution was adjusted to pH 8 with 10 mg mL^{-1} NaOH solution and stored in the refrigerator.

The AgNCs was synthesized according to the reported method with minor modification.[30] Firstly, 0.2 g PVP was first added to 25 mL EG and completely dissolved using magnetic stirring at room temperature. Afterwards, 0.25 g silver nitrate

($AgNO_3$) was added to the PVP solution. Complete dissolution was required to obtain a transparent and uniform solution. Then 6.8 mL of $FeCl_3 \cdot 6H_2O$ solution (2.5mM in EG) was dumped into the mixture and stirred for one or two minutes. The mixture was immediately transferred into a reactor preheated at 130 °C to grow AgNCs for 5 h until the reaction was complete. Finally, acetone and ethanol were used to wash the precipitate with centrifugation of 4000 rpm for 5 min. The AgNCs were re-dispersed in ethanol for future use.

2.4 Preparation of the Chit-GQDs/AgNCs/GE

The gold electrode was polished before each experiment with 1.0, 0.3 and 0.05 μm alumina powder, respectively, rinsed thoroughly in ethanol and double distilled water by ultrasonic alternately. After the gold electrode dried in a stream of nitrogen, 10 μL AgNCs solution was dropped to it and allowed it to dry at room temperature. Then 10 μL mixture of Chit and GQDs (v/v=1:1) was cast on the surface of the gold electrode and left to dry at room temperature to get the Chit-GQDs/AgNCs/GE. The similar procedure was employed to fabricate the Chit/AgNCs/GE and Chit-GQDs/GE.

3. Results and discussion

3.1 Characterization of the prepared GQDs and AgNCs

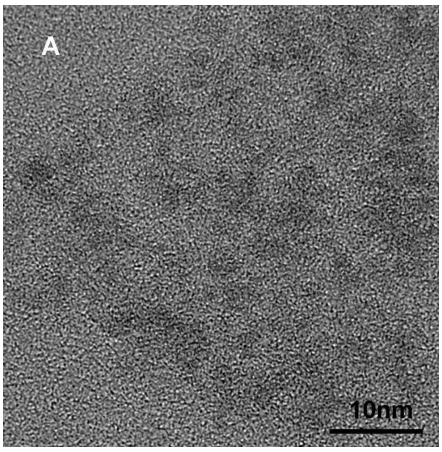

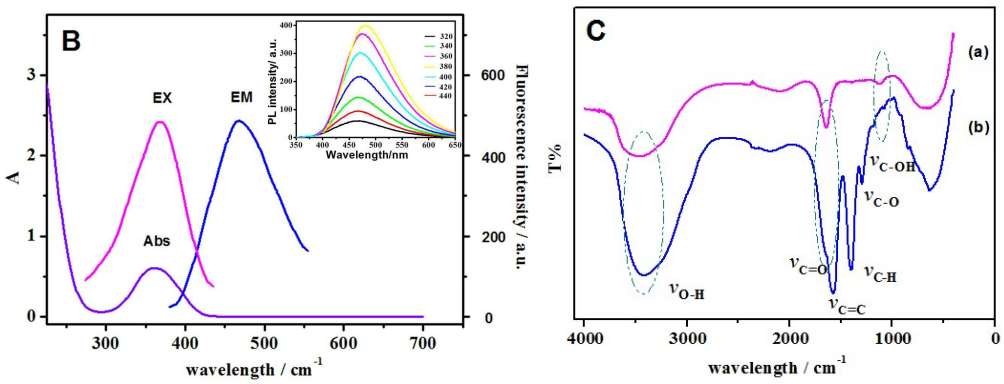

Fig. 1 (A) TEM image of the GQDs; (B) UV-Vis and FL spectrum of the obtained GQDs (Inset: Emission spectra of the GQDs with excitation of different wavelength); (C) FT-IR spectra of citric acid (a) and GQDs (b)

The morphology of the as-synthesized GQDs was characterized by TEM, as shown in Fig. 1A. It can be seen that the GQDs distributed evenly with uniform size of about 2~4 nm. Fig. 1B displays the UV-Vis absorption and Fluorescence spectra of GQDs. As can be seen clearly, the GQDs present a characteristic soret absorption band at about 365nm which is consistent with the previous report of GQDs. [25] Fluorescence spectra historically play an important role in the characterization of GQDs. [31] As shown in Fig. 1B, the emission wavelength of the as-synthesized GQDs is nearly excitation-independent, with the maximum excitation wavelength and the maximum emission wavelength at 362 and 465 nm, respectively. In addition, it can be seen from the inset of Fig. 1B that the maximum PL peak keeps nearly at 465 nm with the change of excitation wavelength from 320 to 440 nm. That is to say, the GQDs have a strong and excitation-independent PL activity. Such excitation-independent PL behavior is related to the GQDs.[32] FT-IR was also used to characterize the obtained GQDs, as shown in Fig. 1C. The GQDs exhibit strong absorption of stretching vibration of C=C at 1600 cm^{-1}, stretching vibration of C=O at 1682 cm^{-1}, C–O at 1240 cm^{-1}, C–H at 1350 cm^{-1} and C–OH at 1112 cm^{-1}, which demonstrate the GQDs maybe contain carboxylic acid groups. Furthermore, the GQDs show absorption of stretching vibration O–H at 3455 cm^{-1}, suggesting that the GQDs contain hydroxyl. [25] Combining the above results of TEM, UV-Vis, FL and FT-IR, we can conclude that the GQDs were synthesized successfully.

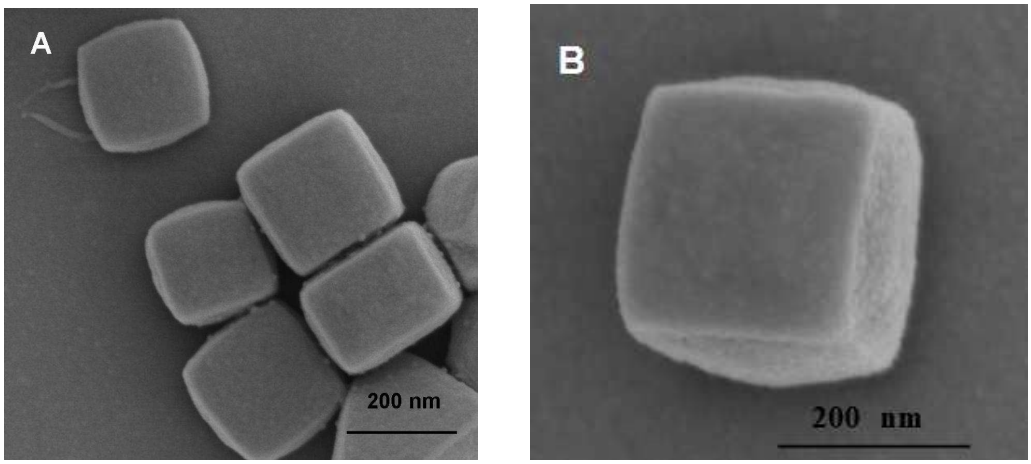

Fig. 2 SEM images of the AgNCs (A) and (B)

The morphology of the as-synthesized AgNCs was characterized by SEM, as shown in Fig. 2A and B. From Fig. 2A, we can find the Ag products mainly consist of small nanocubes with an average edge length of about 200 nm, which exhibits a homogeneous and smooth surface and good dispersion, except for a minority of irregularly shaped particles. Moreover, it can be clearly observed that the AgNCs are well separated from each other which illustrate the AgNCs display good dispersity. Fig. 2B displays amplified image of an independent AgNCs, which can be clearly observed its regular shape and smooth surface of the AgNCs.

Therefore, the combination of the smaller GQDs and the bigger AgNCs will enlarge the active area of the AgNCs and can form synergic effect between the two materials. As such, the composites of GQDs and AgNCs are expected to possess well electrochemical properties and electrocatalytic activity.

3.2 Electrochemical impedance spectroscopy (EIS) characterization

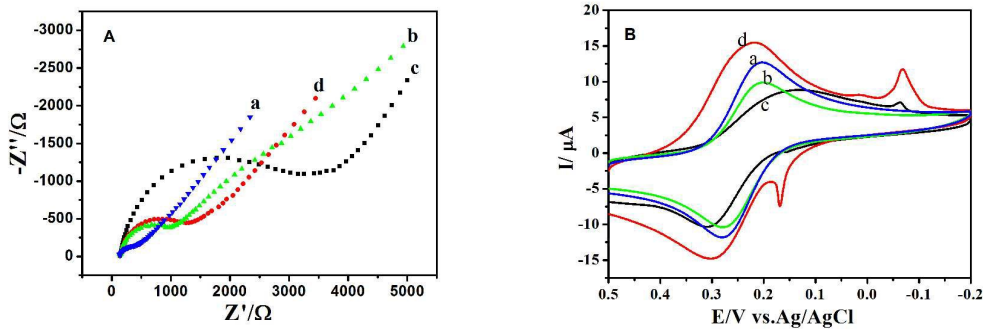

Fig. 3 (A) Electrochemical impedance spectroscopy (EIS) and (B) Cyclic voltammograms (CVs) of: the Bare GE (a), the Chit-GQDs/GE (b), the Chit/AgNCs/GE (c) and the Chit-GQDs/AgNCs/GE (d) in 0.05 M KCl electrolyte solution containing 0.01 M $Fe(CN)_6^{4-/3-}$, the applied ac frequency range for EIS from 0.1 Hz to 100 kHz

EIS has been reported as an effective method to analyze the conductive properties of the electrode surface during the modification process, so we performed the EIS of the different electrodes with a frequency ranging from 0.1 to 100kHz in 0.05 M KCl electrolyte solution containing 0.01 M $Fe(CN)_6^{4-/3-}$, as shown in Fig. 3A. The EIS curve consists of a semicircular part and a linear part. The semicircular part at higher frequencies corresponds to the electron-transfer-limited process and its diameter is equal to the electron transfer resistance (R_{et}). Meanwhile, the linear part at lower frequencies corresponds to the diffusion process. In our experiments, the EIS of the bare GE (curve a of Fig. 3A) displays quite small semicircle diameter, while the Chit-GQDs/GE (curve b of Fig. 3A) and the Chit/AgNCs/GE (curve c of Fig. 3A) exhibit larger semicircle diameter, and the R_{et} are estimated to be 917 Ω and 2837 Ω, respectively. The impedance changes indicate that AgNCs and GQDs have been attached to the electrode surface. Furthermore, the smaller R_{et} of the the Chit-GQDs/GE suggests that the GQDs facilitate well the electron transportation at electrode surface due to its high conductivity. From curve d of Fig. 4A, the R_{et} of the Chit-GQDs/AgNCs/GE is estimated to be about 1240 Ω, which much smaller than that of the Chit/AgNCs/GE. The smaller R_{et} of the Chit-GQDs/AgNCs/GE indicates that the gold electrode modified with GQDs and AgNCs has good conductivity. This should be mainly attributed to the excellent electronic substrate of GQDs which contribute much larger effective surface and more electron transfer passages and thus improve the conductivity of the electrode surface. In a world, the GQDs and AgNCs were successfully immobilized on the electrode and the Chit-GQDs/AgNCs/GE displays good conductivity.

Fig. 3B shows the CVs of the bare GCE, Chit-GQDs/GE, Chit/AgNCs/GE and the Chit-GQDs/AgNCs/GE in 0.1M KCl electrolyte solution containing 0.01 M $Fe(CN)_6^{4-/3-}$. Compared with the bare GE (curve a in Fig. 3B), the Chit-GQDs/GE (curve b in Fig. 3B) and the Chit/AgNCs/GE (curve c in Fig. 3B), the

Chit-GQDs/AgNCs/GE (curve d in Fig. 3B) displays much larger peak currents apparently, which further demonstrates that the Chit-GQDs/AgNCs/GE have a large electroactive surface and can act as a promoter to enhance the electrochemical reaction. In addition, the reduction peak at about -0.05 V of the Chit/AgNCs/GE (curve c in Fig. 3B) and the redox peaks at about -0.05 and 0.16 V of the Chit-GQDs/AgNCs/GE (curve d in Fig. 3B) can be ascribed to the redox of the AgNCs.

3.3 Electrochemical behavior to H_2O_2

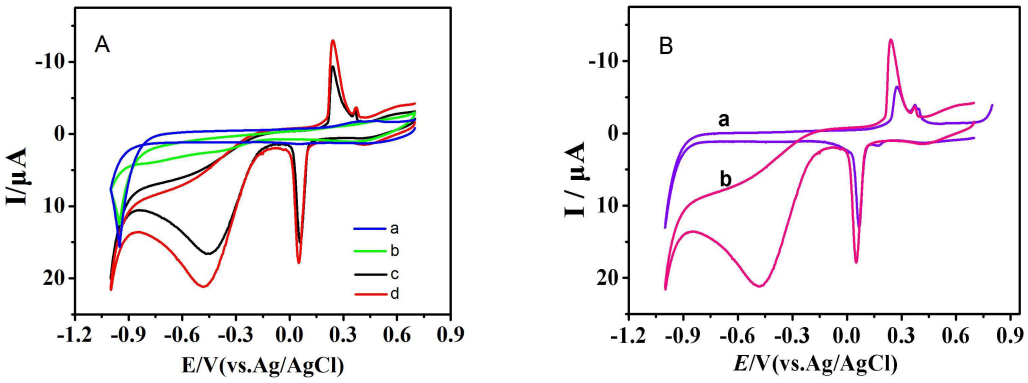

Fig. 4 (A) Cyclic voltammetry (CVs) of the bare GE (a), the Chit-GQDs/GE (b), the Chit/AgNCs/GE (c) and the Chit-GQDs/AgNCs/GE (d) in 0.1 M pH 7.0 PBS containing 1 mM H_2O_2; (B) CVs of the Chit-GQDs/AgNCs/GE in 0.1 M pH 7.0 PBS in the absence (a) and presence (b) of 1 mM H_2O_2, scan rate: 100 mV s^{-1}

To investigate peroxidase-like electrocatalytic activity of the as-prepared Chit-GQDs/AgNCs/GE, we carried out series of CVs experiments. Fig. 4A shows the CVs of the bare GE, Chit-GQDs/GE, Chit/AgNCs/GE and Chit-GQDs/AgNCs/GE in 0.1 M pH 7.0 PBS containing 1mM H_2O_2. No any redox peaks were observed at the bare GE and the Chit-GQDs/GE (curve a and b of Fig. 4A) in the potential range of -1.2~0.9V, and only small background current can be found. To Chit/AgNCs/GE (curve c of Fig. 4A), there presents a pair of redox peaks at 0.0 to 0.3 V and a reduction peak at about -0.45 V. Obviously, the pair of redox peaks at 0.0 to 0.3 V are the characteristic redox of AgNCs.[33] Meanwhile, the reduction peak at about -0.45 V should be ascribed to the electrocatalytic reduction of H_2O_2. The CV of the Chit-GQDs/AgNCs/GE (curve

d of Fig. 4A) presents the same redox peaks as that of the Chit/AgNCs/GE, but the redox peak currents are all bigger than that of the Chit/AgNCs/GE. The results demonstrate that the modified electrodes display similar electrochemical behavior in the presence of AgNCs, but the Chit-GQDs/AgNCs/GE possesses better electrochemical activity under the same condition. The well electrochemical effect of the Chit-GQDs/AgNCs/GE can be attributed to the GQDs, which increase effective surface and provide more electron transfer passages, and then promote the electrochemical performance of AgNCs.

Fig. 4B displays the CVs of the Chit-GQDs/AgNCs/GE in 0.1 M pH 7.0 PBS in absence and presence of 1 mM H_2O_2. Only a pair of redox peaks appear at 0.0 to 0.3 V in 0.1 M pH 7.0 PBS, as shown in curve a of Fig. 4B, which are the characteristic redox peaks of the AgNCs.[33] When added 1 mM H_2O_2 to the 0.1 M pH 7.0 PBS, the CV of the Chit-GQDs/AgNCs/GE presents another remarkable reduction peak at about -0.45 V with bigger peak current, which also proves its good electrocatalytic activity to the reduction of H_2O_2. The well electrocatalytic effect of the Chit-GQDs/AgNCs/GE originates from the AgNCs and the synergistic effect between the AgNCs and the GQDs.

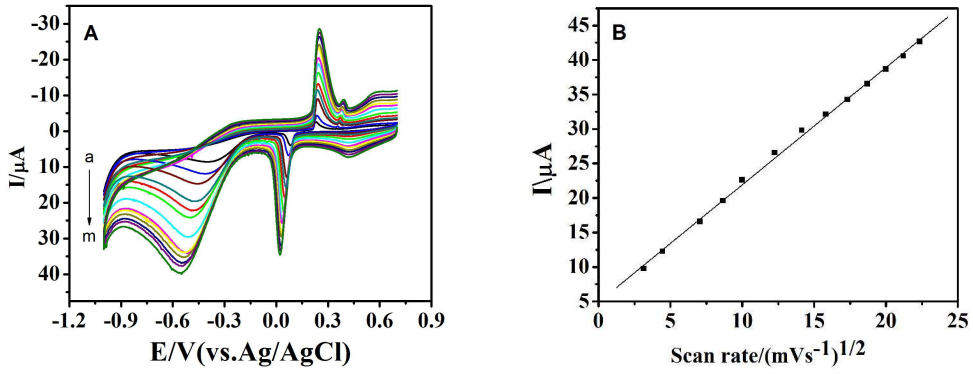

Fig. 5 (A) CVs of the Chit-GQDs/AgNCs/GE in 0.1 M pH 7.0 PBS containing 0.1 mM H_2O_2 at different scan rates, scan rate from a to m are 10, 20, 50, 75, 100, 150, 200, 250, 300, 350, 400, 450 and 500 mVs^{-1}, respectively; (B) Plots of the reduction peak currents at -0.45 V and the square root of the scan rates

To further investigate the electrocatalytic mechanism of the

Chit-GQDs/AgNCs/GE towards H_2O_2 reduction, the effect of scan rates on the voltammetric response was studied. Fig. 5A shows the CVs of the Chit-GQDs/AgNCs/GE in 0.1 M pH 7.0 PBS containing 1 mM H_2O_2 with different scan rates. It is clearly observed that the reduction peak currents at -0.45 V increase obviously with increasing the scan rates. As can be seen in Fig. 5B, the reduction peak currents are linearly proportional to the scan rates in the range from 10 to 500 mVs^{-1}. The regression equation is $I_{pc} = (1.70 \pm 0.02) \times 10^{-6} v^{1/2} + (4.92 \pm 0.34) \times 10^{-6}$ (A, $mV^{1/2}s^{1/2}$, R =0.999). It suggests that the electrocatalytic reduction of H_2O_2 at the Chit-GQDs/AgNCs/GE corresponds to a diffusion-controlled process.

For obtaining the optimal electrochemical response of H_2O_2 at the Chit-GQDs/AgNCs/GE, the effect of pH was also investigated in the pH range from 5.0 to 9.0 (data not shown). The reduction (E_{pc}) peak potential of H_2O_2 shifts negatively with increasing the pH, and the regression equations can be expressed as E_{pc} (V) = – (0.058 ± 0.003)pH – (0.168 ± 0.002) (R = 0.995), indicating that the proton is directly involved in the electrochemical process of H_2O_2. According to the following formula:[34] $dE_p/dpH = 2.303\ mRT/nF$, in which, m is the number of proton, n is the number of electron, and m/n was calculated to be 0.99 for the reduction process, illustrating that the electron transfer is accompanied by an equal number of proton. According to the literature,[35] the corresponding mechanism for electrocatalytic behavior of Chit-GQDs/AgNCs toward H_2O_2 reduction can be deduced as follows:

$$2GQDs\text{-}Ag(0)NCs + H_2O_2 \longrightarrow 2GQDs\text{-}[Ag(1)\text{-}OH)]NCs \quad (1)$$

$$2GQDs\text{-}[Ag(1)\text{-}OH)]NCs + 2e^- + 2H^+ \longrightarrow 2GQDs\text{-}Ag(0)NCs + H_2O \quad (2)$$

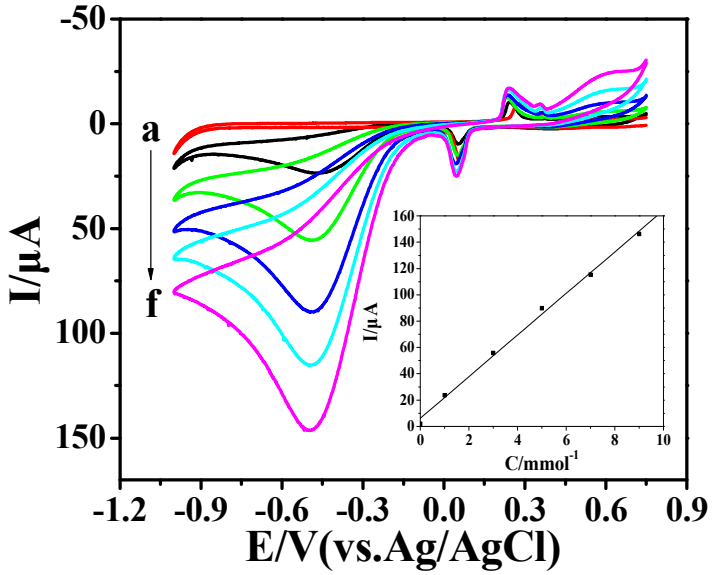

Fig. 6 CVs of the Chit-GQDs/AgNCs/GE in 0.1 M pH 7.0 PBS with increasing H_2O_2 concentration (from a to f: 0, 1, 3, 5, 7, 9 mM); Inset: the relationship between the I_{pc} and the concentration of H_2O_2

Fig. 6 shows the CVs of the Chit-GQDs/AgNCs/GE in different concentrations of H_2O_2 in 0.1 M pH 7.0 PBS at scan rate of 100mVs^{-1}. Obviously, the reduction peak currents increase gradually with increasing the H_2O_2 concentrations (from a to f: 0, 1, 3, 5, 7, 9 mM), indicating a typical electrocatalytic reduction process of H_2O_2. The reduction peak currents increase linearly with the concentrations of H_2O_2, the linearity curve is shown in the inset of Fig. 6.

3.4 Amperometric response to H_2O_2

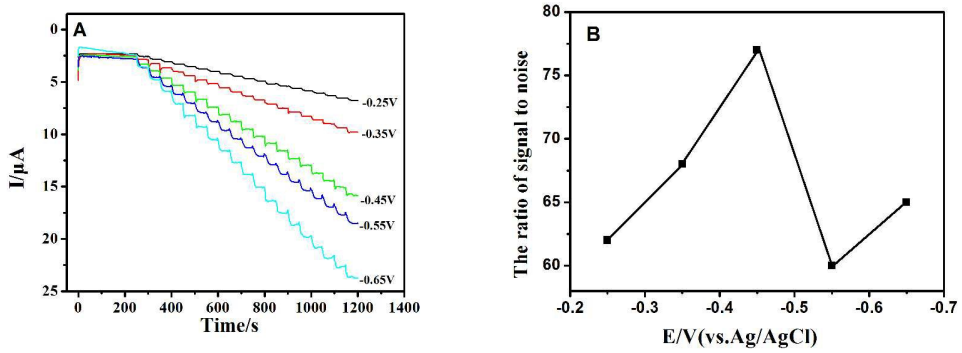

Fig. 7 (A) Amperometric response of the Chit-GQDs/AgNCs/GE with successive additions of 5.0 μL 0.1 M H_2O_2 to 5 mL 0.1 M pH 7.0 PBS at different applied potentials (from -0.25V to -0.65V); (B)

Effect of the ratio of signal to noise on the applied potential

To get a high sensitivity and low noise for H_2O_2 detection and also prevent interference from other electrochemical interfering species, the selection of applied potential in amperometric experiments is very important. Fig. 7A shows the amperometric I-t curves of the Chit-GQDs/AgNCs/GE at applied potentials from -0.25 to -0.65V in 0.1M pH 7.0 PBS with successive additions of 0.1mM H_2O_2. In the potential range from -0.25 to -0.65V, the response currents increase with the decreasing of potential. However, the side reaction takes place on the modified electrode when further decreasing the potential, which results in the increase of background current and inhibition of H_2O_2 reduction at the same time. Notably, the ratio of response current to background current, namely the ratio of signal to noise, increases first and then decreases and the maximum ratio occurs at -0.45V, as shown in Fig. 7B. Therefore, an applied potential of -0.45V was selected as the working potential for further amperometric experiments.

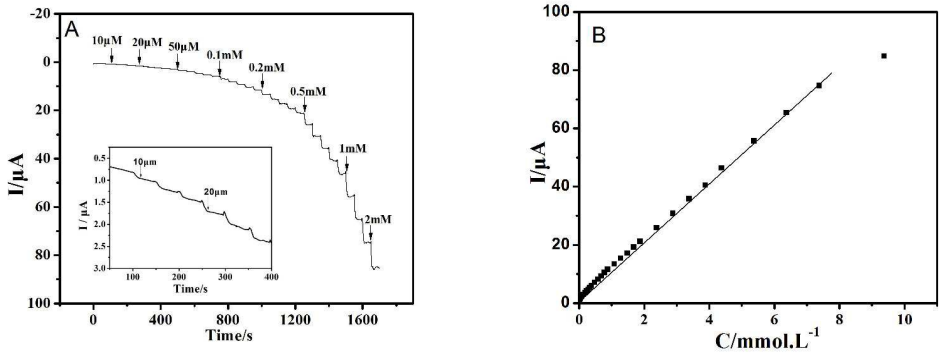

Fig. 8 (A) Amperometric response of the Chit-GQDs/AgNCs/GE to the successive additions of 0.1M H_2O_2 to 5 mL 0.1M pH 7.0 PBS at an applied potential of -0.45V, inset is the blow-up of the low concentration region; (B) Plot of response currents to H_2O_2 concentrations

Table 1 Comparison of the enzyme-free H_2O_2 sensor in our work with the reported H_2O_2 sensors based on AgNPs or other materials modified electrode

Type of electrode	Sensitivity ($\mu A\ \mu M^{-1}\ cm^{-2}$)	Detection limit (μM)	Linear range (mM)	Reference
CQDs/octahedral Cu_2O/	0.130	2.8	0.005–5.3	36

Chit /AgNPs–G/GCE	0.167	7	0.1-10	37
Co_3O_4 nanowalls /GC	0.081	10	0–5.35	38
PVPb–AgNWs	\	2.3	0.02–3.6	39
MWCNT/Ag nanohybrids/GC	0.142[a]	0.5	0.05-17	40
PVP–AgNCs/GCE	\	0.18	0.05-70	41
GQDs/Au electrode	0.051	0.7	0.002-8	27
AgNPs–MWCNT–rGO/GCE	\	0.9	0.1-100	42
Chit-GQDs/AgNCs/GE	0.111	0.15	0.01-7.38	this work

[a] $\mu A\ mM^{-1}$

Fig. 8A displays the steady state amperometric I-t curve of the Chit-GQDs/AgNCs/GE in 0.1M pH 7.0 PBS with successive additions of H_2O_2 at the applied potential of -0.45 V. With successive additions of H_2O_2, the response currents increase in stepwise manner. And an obvious current increase can be observed even the H_2O_2 concentration as low as 10μM (inset in the Fig. 8A). The modified electrode respond immediately after adding H_2O_2 and the time to achieve 95% steady-state current is no more than 8s, indicating a very rapid and sensitive response to H_2O_2. The calibration curve of the response currents and the H_2O_2 concentrations is shown in Fig. 8B, the response currents of the sensor exhibit a linear dependence on the concentration of H_2O_2: I (μA) = (1.93±0.13) + (9.99±0.05)C (mM) (R=0.9996). The sensor displays a linear range from 10 μM to 7.38 mM, with a sensitivity of 141.4 $\mu A.mM^{-1}.cm^{-2}$, and a detection limit of 0.15 μM (S/N=3). The electrochemical performance of this enzyme-free H_2O_2 sensor is comparable or better than those sensors based on AgNPs or electrodes modified with other materials, as shown in Table 1. That is to say, the H_2O_2 sensor based on Chit-GQDs/AgNCs has much superiority, including higher sensitivity, wider linear range, lower detection limit and lower applied potential. The well performance of the H_2O_2 sensor can be attributed to the GQDs which possess good electrochemical performance and the formed synergistic effect between the GQDs and the AgNCs.

3.5 Anti-interference property, stability and reproducibility

In addition, the influence from common co-existing substances on the amperometric response of the Chit-GQDs/AgNCs/GE toward H_2O_2 were also investigated in N_2 saturated 0.1M pH 7.0 PBS. The results exhibit that only an obvious current response can be observed upon the addition of 0.1 mM H_2O_2, and the negligible interferences can be seen after injection of 1mM AA, UA, DA and most ions (K^+, Cl^-, NO_3^-, SO_4^{2-}, Ca^{2+}, Zn^{2+}, Mg^{2+}). The results indicate that the Chit-GQDs/AgNCs/GE exhibits good anti-interference property for H_2O_2 detection.

Stability and reproducibility are two important parameters for electrochemical sensors. In this work, we investigated the stability and reproducibility of the Chit-GQDs/AgNCs/GE by electrochemical method. After the composite membrane electrode was stored in pH 7.0 PBS at 4 °C for 2 weeks, it retained 96.4 % of its original current response, which shows long-term stability. Meanwhile, the relative standard deviation of the sensor response to 0.1 mM H_2O_2 was 2.65 % for 8 successive measurements, which indicate that the H_2O_2 sensor has good reproducibility.

4. Conclusions

In conclusion, a new enzyme-free H_2O_2 sensor was constructed by modifying the synthesized GQDs and AgNCs onto the surface of gold electrode. CV and amperometric experiments indicate that the fabricated sensor displayed well electrocatalytic activity for the H_2O_2 reduction, and it possesses well performance to H_2O_2 detection, such as wide linearity, low detection limit, high sensitivity and selectivity, etc. These experimental results demonstrate that the GQDs and AgNCs are an attractive material for the fabrication of efficient amperometric sensor. The low cost, simple preparation and excellent electrocatalysis properties make the Ag nanocubes a promising candidate for enhanced electrochemical sensing platform.

Acknowledgements

This work was supported by the National Natural Science Foundation of China (No. 21175115), the Program for New Century Excellent Talents in Minnan Normal University (MX14003), and the Innovation Base Foundation for Graduate Students

Education of Fujian Province.

Notes and references

1 S.A. Penkett, B.M.R. Jones, K.A. Brice and A.E.J. Eggleton, *Atmos. Environ.*, 2007, **41**, 154-168.
2 X. Huang, CS. Atwood, MA. Hartshorn, G. Multhaup, LE. Goldstein, RC. Scarpa, MP. Cuajungco, DN. Gray, J. Lim and RD. Moir *et al*, *Biochem*, 1999, **38**, 7609-7616.
3 C. Matsubara, N. Kawamoto and K. Takamura, *Analyst* 1992, **117**, 1781-1784.
4 N.V. Klassen, D. Marchington and H.E. McGowan, *Anal. Chem.*, 1994, **66**, 2921-2925.
5 M.C.Y. Chang, A. Pralle, E.Y. Isacoff and C.J. Chang, *J. Am. Chem. Soc*, 2004, **126**,15392-15393.
6 D.W. King, W.J. Cooper, S.A. Rusak, B.M. Peake, J.J. Kiddle, D.W. O'Sullivan, M.L. Melamed, C.R. Morgan and S.M. Theberge, *Anal. Chem.* ,2007, **79**,4169-4176.
7 P. Vasileva, B. Donkova, I. Karadjova and C. Dushkin, *Colloids Surf. A Physicochem. Eng. Asp.*, 2011, **382**, 203-210.
8 J. Hong, J. Maguhn, D. Freitag and A. Kettrup, *Fresenius J Anal. Chem.*,1998, **361**, 124-128.
9 B. Wang, J.J. Zhang, Z.Y .Pan, X.Q .Tao and H.S.Wang, *Biosens. Bioelectron.*,2009, **24**,1141-1145.
10 S. Chen, R .Yuan and Y. Chai, F. Hu, *Microchim. Acta*, 2013, **180**,15-32.
11 W.Chen, S .Cai, Q.Q. Ren, W Wen and Y.D. Zhao, *Analyst*, 2012, **137**, 49-58.
12 X. Li, X. Liu, W. Wang, L. Li and X. Lu, *Biosens. Bioelectron*., 2014, **59**, 221-226.
13 J. Zhang and J.B. Zheng, *Anal. Methods*, 2015, **7**, 1788-1793.
14 N. Jia, B. Huang, L. Chen, L. Tan and S. Yao, *Sens. Actuators B*, 2014, **195**, 165-170.
15 M.K. Kundu, M. Sadhukhan, S. Barman, *J. Mater. Chem. B*, 2015, **3**, 1289-1300.
16 P. Zhang, C. Shao, Z. Zhang, M. Zhang, J. Mu, Z. Guo and Y. Liu, *Nanoscale*, 2011, **3**, 3357-3363.
17 M. Fang, Z. Chen, S. Wang, H. Lu, *Nanotechnology*, 2012, **23**, 085704.
18 B. Habibi and M. Jahanbakhshi, *Sens. Actuators B*, 2014, **203**, 919-925.
19 Q. Zhang, W. Li, C. Moran, J. Zeng, J. Chen, L.P .Wen and Y. Xia, *J. Am. Chem. Soc.*, 2010, **132**, 11372-11378.
20 Z. Peng and H. Yang, *Nano Today*, 2009, **4**, 143-164.
21 H. Chen, Z. Zhang, D. Cai, S. Zhang, B. Zhang, J. Tang, Z. Wu, *Talanta*, 2011, **86**, 266-270.
22 L.A. Ponomarenko, F. Schedin, M.I. Katsnelson, R. Yang, E.W. Hill, K.S. Novoselov and A.K. Geim, *Science*, 2008, **320**, 356-358.
23 S. Zhu, J. Zhang, C. Qiao, S. Tang, Y. Li, W. Yuan, B. Li, L. Tian, F. Liu and R. Hu, *Chem. Commun.*,. 2011, **47**, 6858-6860
24 J. Shen, Y. Zhu, X. Yang and C. Li, *Chem. Commun.*, 2012, **48**, 3686-3699.
25 J. Peng, W. Gao, B.K. Gupta, Z. Liu, R. Romero-Aburto, L. Ge, L. Song, L.B. Alemany, X. Zhan and G. Gao, *Nano lett.*, 2012, **12**, 844-849.
26 M. Bacon, S.J. Bradley and T. Nann, *Part .Part. Syst. Char.*, 2014, **31**, 415-428
27 Y. Zhang, C. Wu, X. Zhou, X. Wu, Y. Yang, H. Wu, S. Guo and J. Zhang, *Nanoscale*, 2013, **5**, 1816-1819.
28 Ju J, Chen W. *Analytical chemistry*, 2015, **87**: 1903-1910.
29 Y. Dong, G. Li, N. Zhou, R. Wang, Y. Chi and G. Chen, *Anal. Chem.*, 2012, **84**, 8378-8382.
30 J. Jiu, T. Araki, J. Wang, M. Nogi, T. Sugahara, S. Nagao, H. Koga, K. Suganuma, E. Nakazawa, M. Hara, *J. Mater. Chem. A*, 2014, **2**, 6326-6330.
31 K.A. Ritter and J.W. Lyding, *Nature mater*, 2009, **8**, 235-242.

32 Y. Dong, J. Shao, C. Chen, H. Li, R. Wang, Y. Chi, X. Lin, G. Chen, *Carbon*, 2012, **50**, 4738-4743.
33 J.B. Raoof, R. Ojani, E. Hasheminejad, S. Rashid-Nadimi, *Appl. Surf. Sci.*, 2012, **258**, 2788-2795.
34 E. Laviron, *J. Electroanal. Chem. Interfacial Electrochem.* ,1974, **52**, 355-393.
35 M.R. Guascito, E. Filippo, C. Malitesta, D. Manno, A. Serra and A. Turco, *Biosens. Bioelectron.*, 2008, **24**, 1057-1063.
36 Y. Li, Y. Zhong, Y. Zhang, W. Weng, S. Li, *Sens. Actuators B*, 2015, **206**, 735-743.
37 Y. Zhang, S. Liu, L. Wang, X. Qin, J. Tian, W. Lu, G. Chang and X. Sun, *RSC Adv.*,2012, **2**, 538-545.
38 W. Jia, M. Guo, Z. Zheng, T. Yu, E.G. Rodriguez, Y. Wang and Y. Lei, *Journal of Electroanal Chem.*, 2009, **625**, 27-32.
39 X. Yang, J. Bai, Y. Wang, X. Jiang and X. He, *Analyst* , 2012, **137**, 4362-4367.
40 W. Zhao, H. Wang, X. Qin, X. Wang, Z. Zhao, Z. Miao, L. Chen, M. Shan, Y. Fang and Q. Chen, *Talanta*, 2009, **80**, 1029-1033.
41 Y. Wang, X. Yang, J. Bai, X. Jiang and G. Fan, *Biosens. Bioelectron.*, 2013, **43**, 180-185.
42 F. Lorestani, Z. Shahnavaz, P. Mn, Y. Alias, N.S. Manan , *Sens. Actuator B*, 2015, **208**, 389-398.